Organic Process Research & Development **2009,** *13,* 729–738

Process Development for A Novel Pleuromutilin-Derived Antibiotic

Yemane Andemichael, Jun Chen, Jacalyn S. Clawson, Wenning Dai, Ann Diederich, Susan V. Downing, Alan J. Freyer, Peng Liu, Lynette M. Oh,* Daniel B. Patience, Sonja Sharpe, Joseph Sisko,* Julie Tsui, Frederick G. Vogt, Jun Wang, Lori Wernersbach, Edward C. Webb, James Wertman, and Leon Zhou

Chemical Development, GlaxoSmithKline, 709 Swedeland Road, UW2820, PO Box 1539, King of Prussia, Pennsylvania 19406-0939, U.S.A

Abstract:

A scalable synthesis of a novel pleuromutilin-based antibiotic is reported. The synthesis features the scale-up of an interesting skeletal rearrangement of the pleuromutilin core and isolation of a highly purified product despite starting with relatively impure pleuromutilin. The use of Design of Experiment (DoE) and Principal Component Analysis (PCA) tools to achieve these goals is also discussed. Furthermore, the novel coupling of a carbamate and *N*-acyl-imidazole to produce the imidodicarbonate portion of the target molecule is described.

Introduction

Antibiotic resistance is a growing concern in the medical community. The commitment by GSK towards alleviating this problem is exemplified by the research efforts that led to the discovery of compound **1**, a novel pleuromutilin-derived antibiotic. The antibacterial activity of pleuromutilin and its derivatives has been known for more than 50 years,[1] but clinical development of such agents has lagged. In 2007, GSK received marketing authorization for Altabax, itself an agent derived from pleuromutilin, for the topical treatment of impetigo. More recently, compound **1** also showed promising antibacterial properties worthy of further investigation, and this paper describes the chemical process development that enabled its production on larger scale.

The synthetic plan shown below in Scheme 1 was initially employed to make compound **1** (as the succinic acid salt, **1A**) and analogues, and for that purpose it was well-suited.[2] However, for the production of large quantities of **1**, several shortcomings of the route needed to be overcome. Notable among these issues was the desire to avoid phosgene (and its derivatives) to alleviate worker safety concerns, the need to avoid AgOCN due to cost and processing issues, and decreasing the number of isolated intermediates in order to reduce overall costs. Furthermore, the physical properties of a number of the isolated intermediates in this route were suboptimal and rendered large-scale production particularly cumbersome.

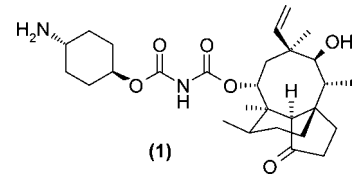

Figure 1. **Compound 1.**

Our search for alternative synthetic routes focused on finding suitable methods to construct the relatively scarce unsymmetrical imidodicarbonate functionality found in **1** without using highly toxic or overly sensitive reagents.[3] Although several possibilities were quickly identified, we focused on that which is described in Scheme 2 because of its brevity, lower cost, and anticipated desirable manufacturing characteristics. This paper describes our efforts to bring these concepts to fruition.

At the outset of our work, several strategic decisions needed to be addressed in order to define the actual isolated intermediates. It was known from the initial scale-up of the chemistry in Scheme 1 that intermediates **3** and **4** were difficult to crystallize and isolate. The natural reflex in this circumstance was to avoid isolation altogether, that is, to convert **2** to **9** without isolation of **3** or **4** (Scheme 2). After only minimal effort it became clear that from a chemistry perspective this approach was quite feasible. However, there were two overriding considerations that forced us to back away from this tactic. First was the recognition that pleuromutilin (**2**) is a fermentation product, and batches of **2** that arrived in our laboratories for process development contained no less that 35 different impurities, the structures of which were mostly unknown. While there was an expectation that the fermentation, crystallization, and isolation processes would ultimately be optimized so as to reduce the variability and amounts of the impurities found in **2**, we reasoned that the crystallization and isolation of additional intermediates from Scheme 2 would help to secure the necessary and consistent purity of **1A**. Second, feedback from our manufacturing partners within GSK indicated that the benefits derived from avoiding the isolation of sequential intermediates would be offset by the increased reactor residence time and an overall decrease in 'process velocity'.

* Authors for correspondence. E-mail: lynette.m.oh@gsk.com. Telephone: 610-270-5492. Fax: 610-270-4829. E-mail: joe.sisko@gsk.com. Telephone: 610-270-4360. Fax: 610-270-4829.

(1) Kavanaugh, F.; Hervey, A.; Robbins, W. J. *Proc. Natl. Acad. Sci. U.S.A.* **1951**, *37*, 570.

(2) Brook, G.; Burgess, W.; Colthurst, D.; Hinks, J. D.; Hunt, E.; Pearson, M. J.; Shea, B.; Takle, A. K.; Wilson, J. M.; Woodnutt, G. *Bioorg. Med. Chem.* **2001**, *9*, 1221.

(3) For literature methods of preparing imidodicarbonates, see: Itoh, T.; Watanabe, M.; Fukuyama, T. *Synlett* **2002**, *8*, 1323. Hajra, S.; Bhowmick, M.; Maji, B.; Sinha, D. *J. Org. Chem.* **2007**, *72*, 4872. Singh, O. V.; Han, H. *Org. Lett.* **2007**, *9*, 4801. Hageman, H. *Angew. Chem., Int. Ed. Engl.* **1977**, *16*, 743. Gorbatenko, V. I. *Tetrahedron* **1993**, *49*, 3227.

10.1021/op900104g CCC: $40.75
Published on Web 07/02/2009

Scheme 1. **Original synthesis of compound 1A**[a]

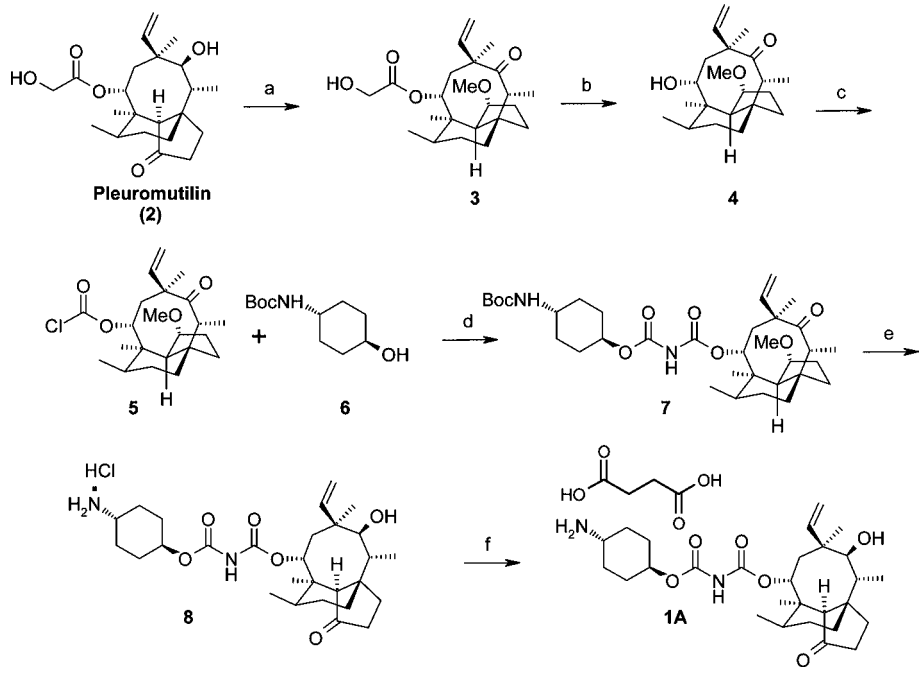

[a] Reagents and conditions: (a) $(CH_3O)_3CH$, MeOH, H_2SO_4, 30 °C; (b) KOH, MeOH, H_2O, 65 °C; (c) THF, pyridine, triphosgene, H_2O, CH_2Cl_2; (d) CH_2Cl_2, cat. pyridine, AgOCN; (e) EtOAc, HCl, NH_4OH to pH = 5; (f) CH_2Cl_2, aq K_2CO_3, 1-PrOH, succinic acid.

Scheme 2. **Improved route to compound 1A**[a]

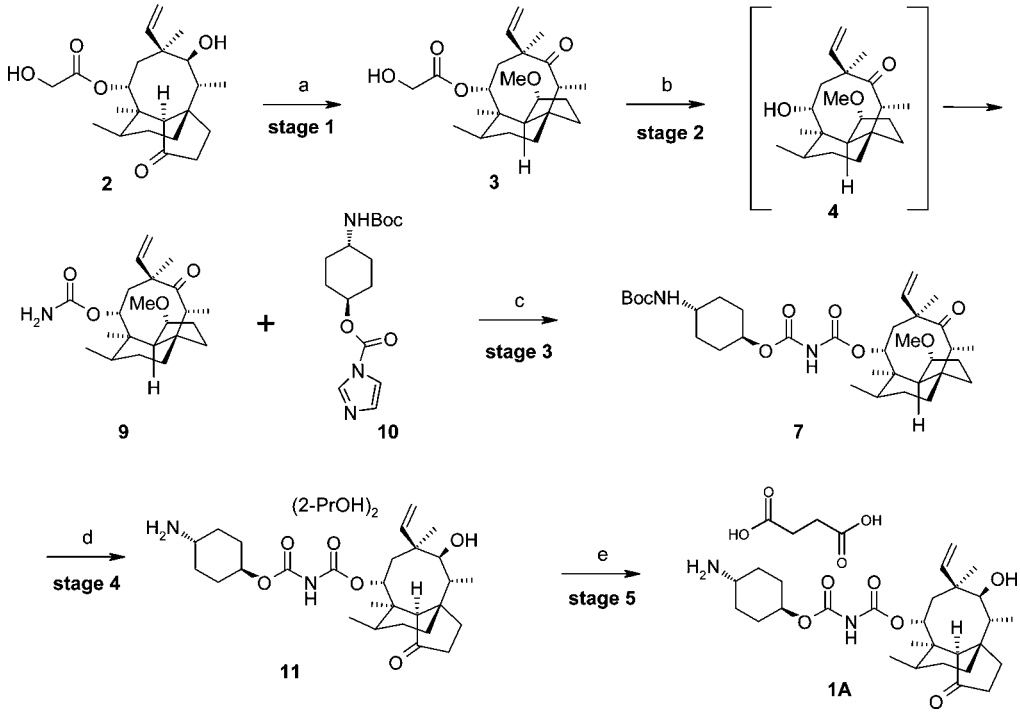

[a] Reagents and conditions: (a) $(CH_3O)_3CH$, MeOH, H_2SO_4, 72−77%; (b) MeOH, aq KOH, heptane, *tert*-butyl methyl ether, chlorosulfonyl isocyanate, Et_3N, H_2O, toluene, 85%; (c) *N*-methyl pyrrolidinone, NaO-*tert*-pentoxide, aq citric acid; (d) toluene, HCl, aq NH_4OH, 2-PrOH, EtOAc, 83% for 2 steps; (e) 2-PrOH, H_2O, succinic acid, 92%.

After re-examining our plan it was felt that **4** would be the best intermediate to isolate, since any method for converting **3** to **4** would require aqueous conditions, but the subsequent conversion of **4** to **9** would almost certainly require anhydrous conditions. Hence, isolation and drying of **4** prior to conversion to **9** seemed logical. In practice, the conversion of **2** to **4** without isolation of **3** was actually quite simple to accomplish with good overall yields. However, despite significant efforts, we simply could not develop a reliable process for the crystallization of **4**. As such we refocused our efforts on the isolation of **3** followed by the conversion of **3** to **9** without isolation of **4**.

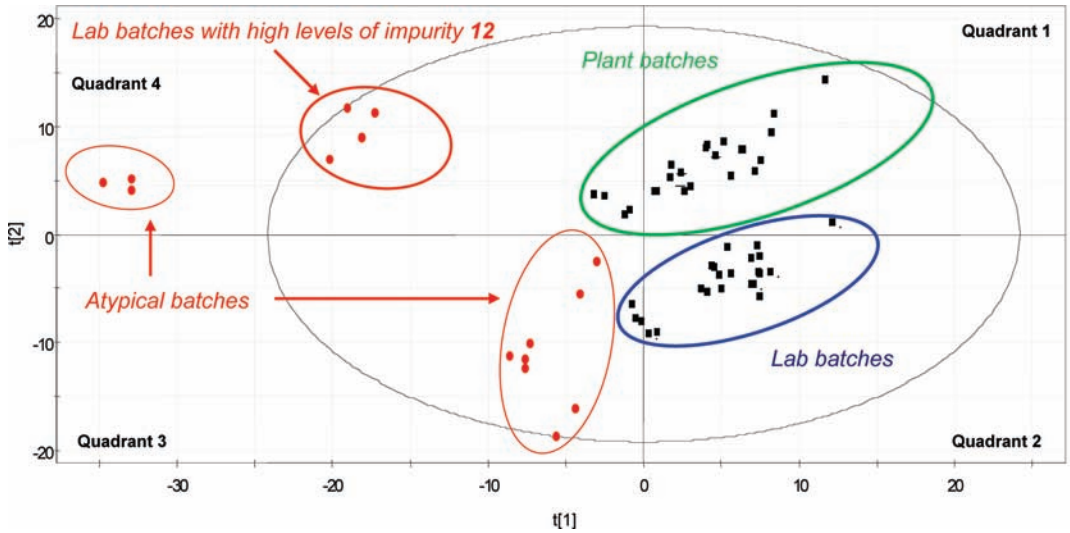

Figure 2. **PCA score plot of IR spectra of batches of pleuromutilin 2.**

As noted above, production of pleuromutilin (**2**) is accomplished by a complex fermentation process, followed by extraction with an organic solvent and subsequent crystallization. However, a practical limitation of this process is that batches of **2** contained varying amounts of approximately 35 individual impurities, the structures of which were mostly unknown and difficult to accurately quantify due to their low concentrations and poor UV absorbances. The complex impurity profile of **2** made it difficult to set a conventional specification for quality control. Principal component analysis (PCA) is a powerful technique[4] of identifying patterns in data and expressing the data in such a way as to highlight their similarities and their differences, i.e., impurity profiles. We decided to conduct a study of the variability in the purity of **2** using multivariate analysis of the diamond attenuated total reflectance (DATR)/IR spectra from various batches. DATR/IR is a rapid, less time-consuming technique than our HPLC method, enabling dozens of analyses to be collected in a short amount of time. The IR spectra were collected on three replicates from each batch, and principal component analysis was performed on these spectra.[5] The PCA score plot of lab and plant batches of **2** is shown in Figure 2.

Each data point in the score plot represents one sample spectrum. These data points are grouped in the plot based on their relative similarities and differences. The proximity of the data points situated in the plot indicates similarity of batches of **2** in terms of overall purity and impurity content. A number of distinct clusters can be discerned. The horizontal axis (the first principal component) in the plot corresponds primarily to the content of **2**, with batches to the right (quadrants 1 and 2) having higher level of purity. The second principal component, as represented by the vertical axis, is believed to reflect the variation of some of the impurities residing in the batches. Lab and plant batches from the typical fermentation process (higher purity) are in two separate clusters; both of which are found in quadrants 1 and 2. Lower-purity batches, such as those produced from "atypical" fermentation processes (where the feedstock was altered), or batches containing high levels of impurity **12** (Scheme 3) are clustered to the left in quadrants 3 and 4. Thus, it was encouraging to us that the DATR/IR data used in combination with PCA techniques were correlating to HPLC purity profiles. Despite the high variability and complexity of the purity of **2**, the technique grouped batches of **2** based on their overall purity and impurity profile, making it easier for visualization. More importantly, it allowed us to begin identifying which batches were acceptable for use, thus helping us toward our goal of setting specifications. One of those studies is described here. As mentioned previously, impurity **12** (Scheme 3) is a prominent impurity which varied in amounts ranging from 1 to 25%. In order to understand how the variable amounts of **12** might impact on the stage 1 process, an online DATR/IR method was developed to monitor the kinetics of this chemistry.[6] IR data from two reactions which utilized batches of **2** situated in different quadrants (second vs fourth) in the PCA score plot (Figure 2) were evaluated to gain

Scheme 3. **Convergence of 2 and impurity 12 to intermediate 4**

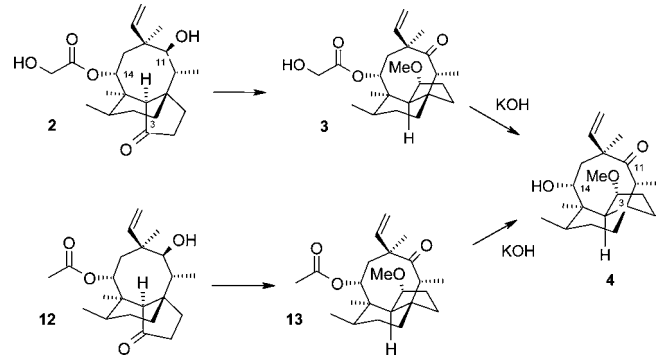

(4) For a leading reference on PCA see: Eriksson, L.; Johansson, E.; Kettaneh-Wold, N.; Wold, S. *Multi- and Megavariate Data Analysis*; Umetrics Academy: Umea, Sweden, 2001.

(5) *Umetrics SIMCA-P*, version 11multivariate data analysis software was used in this study. The DATR-IR data were collected using a Smiths Detection (Danbury, CT) FT-IR spectrometer equipped with a diamond attenuated total reflection (DATR) sampling interface. The IR spectral data in the range from 800 to 1800 cm^{-1} were normalized by regressing it against the average spectrum, and the resultant (filtered) data were subjected to the PCA analysis.

(6) The in situ infrared data were collected using Mettler-Toledo AutoChem (Columbia, MD) MonARC Process IR with Neotecha recirculation sampling loop. .

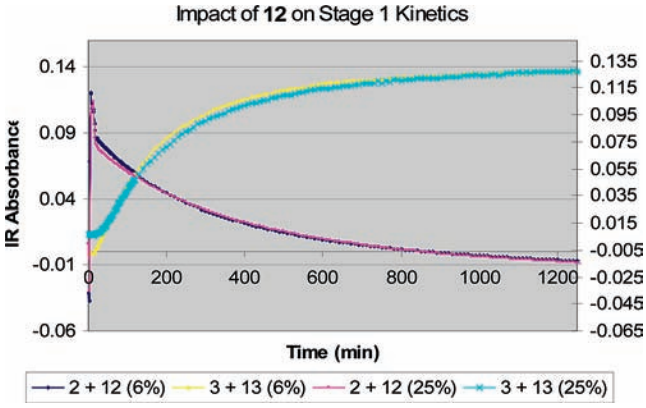

Figure 3. **Stage 1 online IR profiles.**

understanding of the extent of the impact. These two reactions were conducted using batches of **2** that contained approximately 25% and 6% of acetate **12**, respectively. The reaction profiles are overlaid in Figure 3. The superimposable profiles for both the consumption of starting materials and the formation of product indicate these two reactions proceeded at virtually the same reaction rate from the beginning to the end. Therefore, the presence of **12** at levels as high as 25% in batches having different impurity profiles does not have much impact on the outcome of the reaction.

Concurrently, it was shown that **12** was converted to **13** in stage 1, and we reasoned that the stage 2 hydrolysis would render this problem moot as **3** and **13** should both be converted to **4**. In contrast, little was known about the structures of the remaining impurities which greatly complicated the data analysis during our studies to optimize the conversion of **2** to **3** (*vide infra*).

The strategic choice for the stage 1 conversion of **2** to **3** was made to 'protect' the alcohol at C-11 while allowing for selective manipulation at the latent hydroxyl group on C-14. Although this reversible process had previously been reported,[7] the practical challenges brought on by the variable purity profile of **2** made it difficult to optimize this reaction and ensure its robustness. The mechanism for the formation of **3** is believed to involve a number of discrete steps including epimerization and corresponding ring flip at the cyclopentane junction of **2** followed by oxonium ion formation at C-3 under conditions which promote ketalization. Finally, a stereospecific hydride transfer from C-11 to C-3 produces **3**. Ensuring that these steps occur while controlling competitive product degradation under the reaction conditions made this a challenging process to optimize.

Reaction Optimization

We began by conducting sequential design of experiment (DoE) studies of the variables and factors which we believed would influence the yield and purity profile of the reaction (Table 1).

The initial half factorial designs indicated that there was significant curvature in the linear responses that merited further investigation. Moreover, the analysis of the reaction space also suggested that the reaction optimum may be outside of the initial

Table 1. **Factor set points and ranges for stage 1**

factor	initial set-points	ranges (half-factorial study)	ranges (RSM study)
MeOH	4.2 vol	2.0−6.0 vol	4.0−8.0 vol
H_2SO_4	0.3 vol	0.1−0.5 vol	0.05−1.0 vol
trimethyl orthoformate (TMOF)	1.6 vol	0.6−2.0 vol	0.4−1.6 vol
temperature	30 ° C	20−40 ° C	0−40 ° C

Scheme 4. **Formation of impurity 14 from 3**

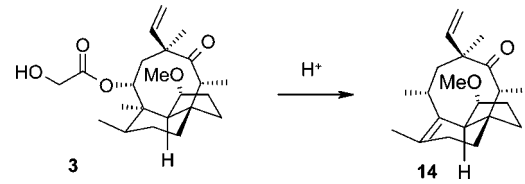

ranges. Additional runs at wider dilutions and temperature settings established the ranges for the subsequent response surface modeling (RSM) study.[8] We elected to generate a response surface model using a central composite design, the main goals of which were to maximize conversion to **3** during extended hold periods (up to 24 h) and to obtain a reaction mixture with an impurity profile that would perform well in the isolation procedure (*vide infra*). Principally, we were most concerned with maximizing the consumption of the starting material **2** and minimizing the formation of the major impurity, identified as alkene **14** (Scheme 4), since both had proved difficult to purge.

To maximize production of **3**, the most important factors were temperature and an interaction between H_2SO_4 volumes and temperature. Lower temperatures and lower acid amounts should produce more of the product (**3**) (Figure 4). Note also that, at lower acid amounts (e.g., 0.25 vol), the gentler slope suggests less variation in the amount of **3** produced across the temperature range and therefore would likely be a more robust process in the event of temperature excursions on scale up.

Similarly, reactions conditions with (a) higher temperatures and less acid or (b) lower temperatures and more acid would minimize the amount of starting material **2** remaining (Figure 5).

The RSM also indicated that the interaction between H_2SO_4 volumes and temperature (Figure 6) was most influential on

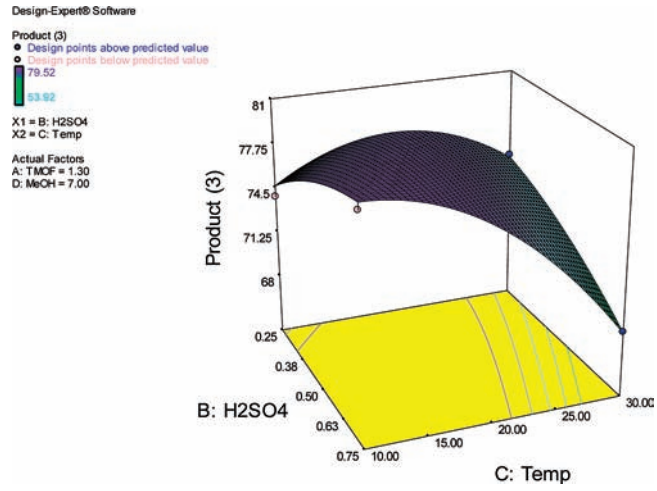

Figure 4. **Effect of interaction of H_2SO_4 and temperature on product (3) levels.**

(7) Berner, H.; Schulz, G.; Schneider, H. *Tetrahedron* **1980**, *36*, 1807.

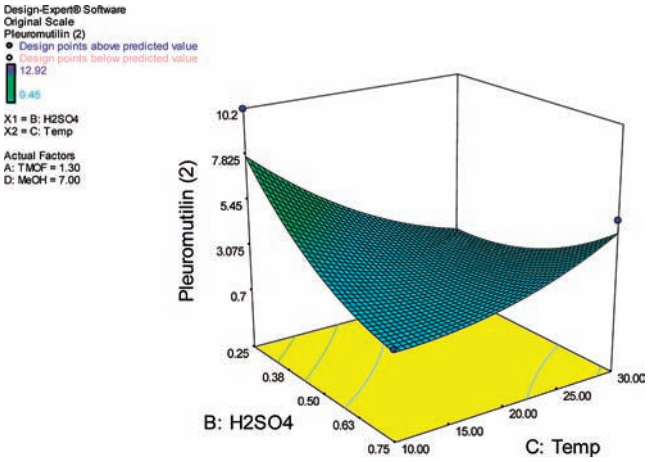

Figure 5. **Effect of interaction of H_2SO_4 and temperature on pleuromutilin (2) levels.**

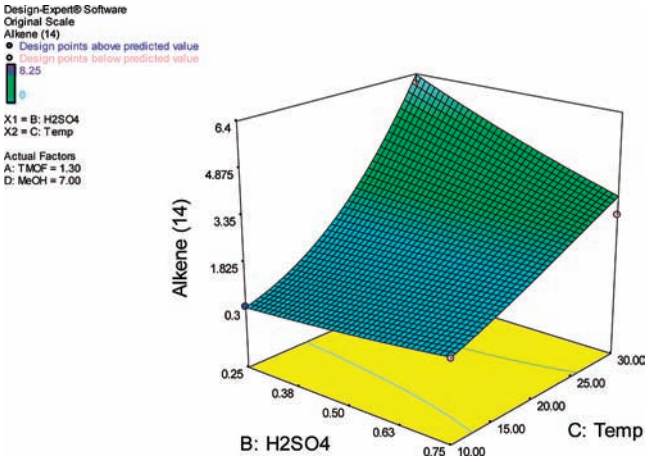

Figure 6. **Effect of interaction of H_2SO_4 and temperature on alkene 14 levels.**

the level of alkene **14** generated. At lower temperatures, the level of the alkene impurity **14** remained relatively low and constant over the range of acid volumes, while at higher temperatures the level of impurity **14** increased more significantly (Figure 6).

Recalling that all these optimization studies were conducted based on a 24 h reaction time and that data from our crystallization work (*vide infra*) indicated that approximately 4% of the alkene **14** and 3% of pleuromutilin **2** could be purged, an operating range was defined to maximize yield and achieve our purity targets (Figure 7).

The major conclusion from the central composite study is that, in order to maximize product formation while minimizing the amounts of **2** and **14** to levels that could be comfortably purged by our crystallization protocol, less acid (0.25 volumes), lower temperature (25 °C), and 7 volumes of MeOH with 1.3 volumes of TMOF should be employed. Importantly, our initial plant runs at 40 kg scale confirmed these results. Two successive runs at 25 °C required 24 h to reach completion and gave isolated yields of 79% and 75%, both with >97% purity by HPLC. With the goal of improving our process velocity, additional studies also indicated that reaction times could be significantly shortened to 6−7 h by conducting the reaction at

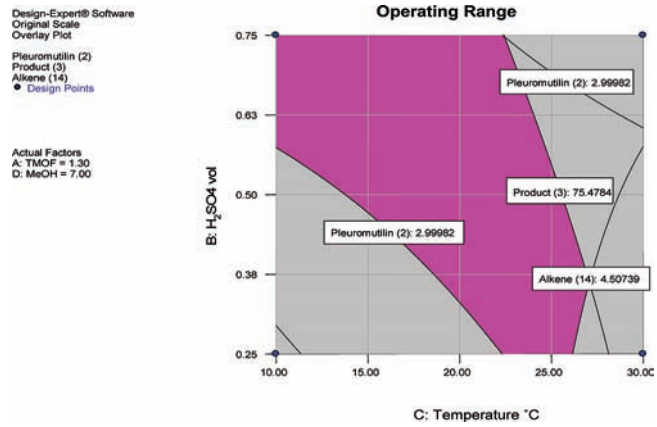

Figure 7. **Operating range for H_2SO_4 charge and temperature.**

35 °C with no loss in purity.[9] We were gratified to confirm these predictions with three additional plant runs at 40 kg scale that produced 72−77% isolated yields with nearly impurity profiles identical to those above. The slightly lower-yielding reaction was a direct result of using a batch of **2** that was 3−4% less pure than those used in the other runs.

Crystallization Development

Since the solvent for stage 1 was methanol, crystallization development began by investigating water as an antisolvent. The original route (Scheme 1) utilized water as an antisolvent to precipitate **3**, but due to limited development work at that time, the process had isolation issues on the initial scale-up to 15 kg. Therefore, redevelopment of the crystallization began with solubility studies of purified **3** in varying ratios of methanol and water at 25 °C. This investigation revealed a new crystalline form of **3** that was confirmed by microscopy and thermal analysis[10] (Figure 8). Ripening experiments with this sample as seed material yielded a pure sample of the new form. Along with its higher melting point, this ripening suggested that the new form was the more stable of the two forms. The habit of the new crystal form (bladed) was also more desirable than that of the original form (acicular) because the needle-like (or acicular) crystals gave poorly mixing slurries and difficult filtrations. Accordingly, ongoing development had the added focus of maintaining form control to isolate the newly discovered form.

The solubility was measured gravimetrically at three ratios of methanol and water and four temperatures. This enabled a seeded cooling crystallization in which water is added to the methanol solution to saturate the solution at the desired seeding temperature prior to adding seeds. Scaling the process to a 1-L vessel revealed two issues−slight oiling prior to seeding and sudden nucleation of the undesired form during the cooling profile. Analysis of the oil phase showed that it was primarily

(8) *Design-Expert*, version 7.0.3; Stat-Ease, Inc.: Minneapolis, Minnesotawas used to analyze the data. The study type was a response surface modeling based on central composite design (30 experiments). Overlay plot (operating range) was generated using graphical optimization technique.

(9) Presented by James Wertman at the Dynochem User Group Meeting 2007, May 15−16, 2007, Philadelphia PA.

(10) This data was collected on a TA Instruments 2920 DSC, with a 10 °C/min temperature ramp rate.

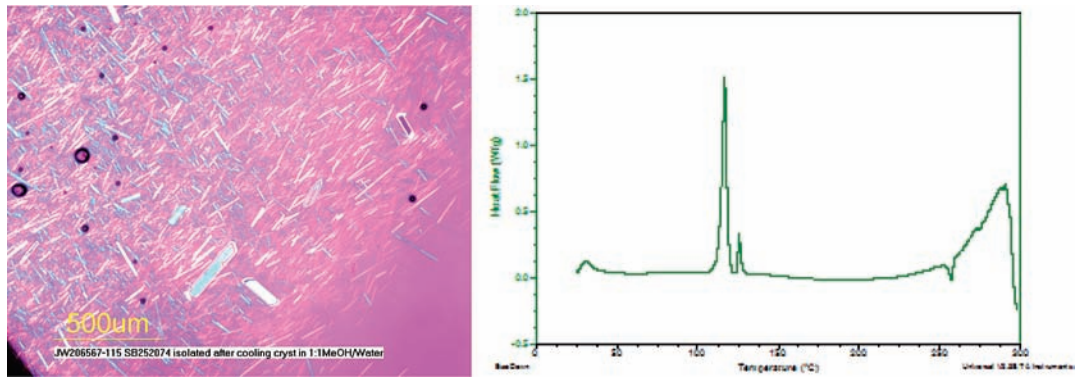

Figure 8. **Microscopy and thermal analysis of the new form of 3.**

acetate impurity **13**. We quickly found that for reactions with >5% of **13**, the addition of 5−10% of methyl isobutyl ketone limited the impact of **13** on the crystallization by preventing this oiling and minimized the amount of **13** found in the isolated product.

With regards to nucleation of the undesired form, several methods were tested to improve the form control and suppress nucleation, including increased seed loading, improving the chemical and form purity of the seeds, and changing from a dry addition to a slurry addition of seeds. However, the most significant improvement was through the modification of the cooling profile. Although the seeding temperature was not changed, a longer hold time after seeding was implemented to ensure complete desupersaturation. It was also determined that a cooling rate of <0.10 °C/min after this hold time was required to prevent nucleation of the undesired form. In the event of an unsuccessful form control, it was also determined that a ripening of the solution could convert the product completely to the desired form. This was a crucial contingency, considering that the undesired form yielded a compressible product cake with a cake resistance 2 orders of magnitude larger than the desired form, which led to excessively long filtration times. Careful attention to the temperature control and cooling rate on scale-up prevented the need to employ the ripening protocol for any of the batches, and only small amounts of the undesired form could be observed in in-process samples. The key signal of success of the crystallizations was the smooth isolations by centrifugation (which can exacerbate poor filtrations through excessive cake compression). No operation issues were observed, and the filtration time was as predicted for the desired form. Also, in line with expectations was an average adjusted yield of 84% and total impurity levels <3%, despite impurity levels ranging from 5 to 17% in the input material.

Having secured a relatively robust and efficient manner of obtaining highly pure product **3**, the remainder of the synthesis became considerably less complex. As noted above, obtaining anhydrous **4** was deemed imperative since we expected conversion to **5** would utilize water-sensitive reagents. Towards this goal, we examined the hydrolysis of **3** to **4** under phase transfer conditions in toluene. In fact, hydrolysis of **3** (and to some extent **13**) could be achieved with Bu_4NCl (3%) and aqueous KOH in high yield, while formation of the unexpected impurity **15** was kept to <1% (Scheme 5).

While the extractive workup of **4** in toluene followed by azeotropic removal of water permitted an isolation-free process

Scheme 5. **Base-mediated formation of impurity 15**

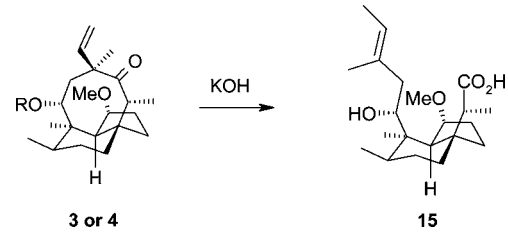

3 or 4 **15**

to provide anhydrous intermediate **4**, problems with emulsions in the plant forced us to develop a more efficient transition to the carbamoylation step. In the revised procedure, alcohol **3** was heated in aqueous KOH in MeOH to induce hydrolysis followed by an extraction of **4** into heptane and an azeotropic distillation to remove any residual water. Slow addition of chlorosulfonyl isocyanate (CSI) to the heptane solution of **4** generated intermediate **16** which was hydrolyzed to **9** by treatment with water and triethylamine in high yields and consistently high purity after isolation by crystallization (Scheme 6). Once again our plant results closely matched the lab results. Four consecutive runs at 24 kg scale provided **9** in isolated yields of 77−87% with purities all exceeding 99% by HPLC.

Completion of the synthesis required only the coupling of **9** and **10**[11] to produce **7** followed by acid-mediated conversion to **11** (Scheme 7). The choice of solvent for these transformations was deemed critical due to the poor solubility of **10** in most solvents and the desire to use a solvent during the conversion of **7** to **11** that was inert to strong acids like HCl. The coupling reaction was initially run by combining **9** and sodium *tert*-pentoxide (2.5 equiv) in 10 volumes of THF at 0−5 °C for 5−10 min, followed by addition of portions of **10** as a solid. Although this gave acceptable yields in our initial plant campaign, there were several aspects of this chemistry that we wanted to explore. First, we wondered if this transformation could be accomplished with a milder base that did not require strictly anhydrous conditions. Next, we wanted to find a means of adding the base as a solution or suspension because addition of sodium *tert*-pentoxide as a solid clogged the hopper and lines in the plant. Finally, we looked to find a solvent that was capable of making stable

(11) Compound **10** was readily prepared in high yield from commercially available trans-4-aminocyclohexanol by sequential treatment with di-*tert*-butyl dicarbonate (Boc2O) and *N*,*N*′-carbonyldiimidazole (CDI).

Scheme 6. **Conversion of alcohol 4 to carbamate 9**

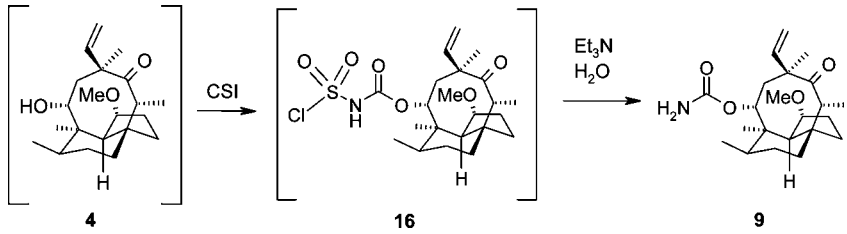

4 **16** **9**

Scheme 7. **Formation of intermediate 11**

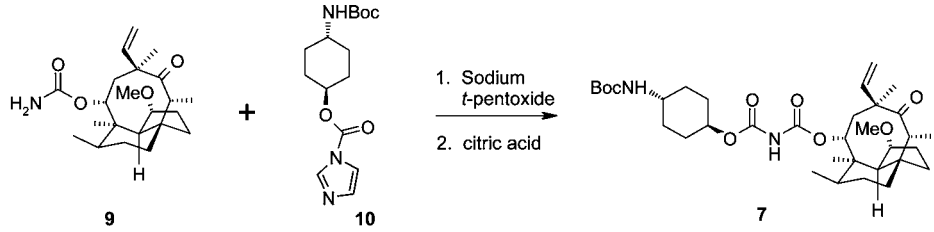

9 **10** **7**

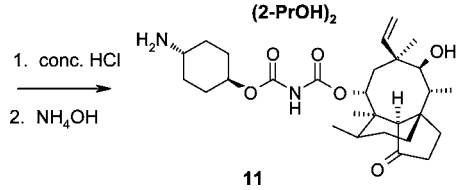

11

solutions or suspensions of the base, providing high yields of the product and also leading to a simple workup.

An initial base screen confirmed that bulky alkoxide bases such as sodium *tert*-pentoxide provided the best conversions, while weaker inorganic bases (K_2CO_3, K_3PO_4) gave no conversion at all. Furthermore, NMP was found to be a superior reaction solvent that also allowed for a much simpler process. Dissolving sodium *tert*-pentoxide in 2 volumes of NMP allowed for a controlled addition of base to a homogeneous mixture of **9** and **10** that had been dissolved in 3 volumes of NMP and cooled to 5 °C. After 30 min, the product (as its sodium salt) could be precipitated by adding the reaction mixture to a large excess of water. Because the sodium salt of **7** readily deliquesced upon storage for a few days, we added citric acid to the water quench to produce a buffered system at pH 4 that smoothly precipitated **7** as a fine white powder that could be easily stored. Two runs at 40 kg scale produced excellent results with very high purity and isolated yields of **7** estimated to be >90% that were used directly in the next step without drying.

We had envisioned toluene as the ideal choice for the conversion of **7** to **11** because of its chemical stability towards conc HCl and because it was expected to provide a clean phase separation from the aqueous phase after reaction completion. Indeed, we found that simply mixing **7** in toluene (4 volumes) followed by a water wash to remove any residual NMP from the previous step, then adding 1.5 volumes of conc. HCl at 15 °C for ∼4 h smoothly produced **11** with high conversions (Scheme 8). The Boc group was typically cleaved in the first 30−60 min, at which point the primary amine intermediate **17** became fully soluble in the aqueous layer. Stirring for a

Scheme 8. **Formation of 11 via intermediate 17**

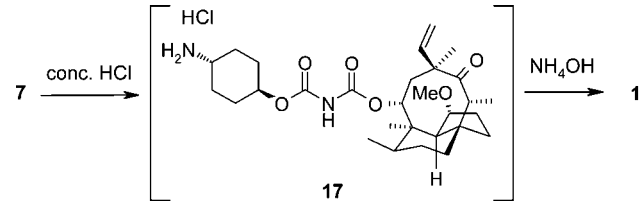

17

few additional hours effected the skeletal rearrangement to produce **11** as the HCl salt. Separating the toluene phase efficiently removed any nonpolar impurities that formed during the reaction while retaining the product in the aqueous acid layer. Isolation of the free base of **11** involved slow addition of the aqueous layer to a mixture of ammonium hydroxide and EtOAc to which 2-PrOH had been added. After removing the bottom aqueous layer, a solvent exchange into 2-PrOH followed by a seeded, cooling crystallization produced crystalline **11** in high yields and purity. It is interesting to note that, while 2-PrOH was the crystallization solvent due to the modest solubility of **11** in this solvent, its presence in the EtOAc extraction was essential for efficient extraction from water. Once again, the plant runs at 65 kg scale gave highly pure product and yields of >80% of **11** over 2 steps.

The final step in the sequence involved formation of the succinic acid salt (**1A**). Initial salt screening of compound **1** revealed that crystalline succinic acid salts could be made both with a 1:1 and 0.5:1 (succinic acid: **1**) stoichiometry.[12,13] From the outset it was presumed that the 1:1 stoichiometry would be easier to control, and so this became our target. In addition, the high aqueous solubility of both salts (>10 mg/mL) suggested that

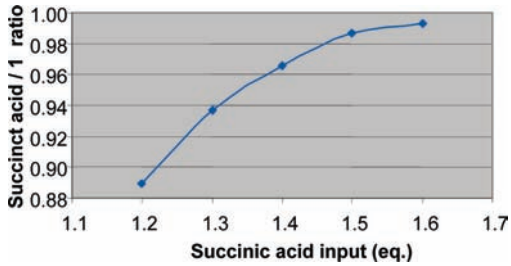

Figure 9. **Salt ratios of 1A as a function of succinic acid input.**

physical properties of the API, such as particle size, would not likely become critical quality attributes and that manufacturing attributes would dominate our selection criteria.

Solubility data from a solvent screen in combination with the results from a preliminary polymorph screen identified 1-PrOH as the initial solvent of choice. However, high residual 1-PrOH levels (9−12%) were found in our first scale-up batches of API after drying for 24−30 h. The choice of solvent was later re-evaluated, and a 2-PrOH/H_2O system (9:1) was shown to give the product that was the same form by XRPD and contained less residual solvent (0.5−2%) after drying for 24 h.

A study was conducted to optimize the required succinic acid charge to ensure the reproducible formation of the 1:1 salt, **1A**. The results showed that in 9:1 2-PrOH /H_2O, at least 1.6 equiv of succinic acid was needed to prepare **1A** (Figure 9). Because of its high water solubility, the process for making **1A** involved initial dissolution of **1** in a 4:1 ratio of 2-PrOH/water (2.5 volumes) with 1.6 equiv of succinic acid. This mixture was heated until complete dissolution followed by a final clarifying filtration of the product. Subsequent additions of 2-PrOH as the antisolvent and slow cooling led to a high-yielding and controlled process for production of **1A**. The scale-up of this process to 2 kg proceeded uneventfully to give the final API in 92% isolated yield with >99% purity.

Conclusion

A scalable synthesis of the novel pleuromutilin-based antibiotic **1A** was developed. The synthesis features the scale-up of an interesting skeletal rearrangement of the pleuromutilin core and isolation of a highly purified product despite starting with relatively impure pleuromutilin. Furthermore, the novel coupling of a carbamate **9** and *N*-acylimidazole **10** to produce the imidodicarbonate portion of **1** is described and optimized. The route has been scaled up in plant to produce high-quality API.

(12) A salt with a ratio of 2:1 (succinic acid:**1**) could also be formed via the liquid-assisted drop grinding technique, but as this technique is limited to lab-scale preparations, it was not considered a viable option for scale-up. For details of the liquid-assisted drop grinding technique, see: Friscic, T.; Trask, A. V.; Jones, W.; Motherwell, W. D. *Angew. Chem., Int. Ed.* **2006**, *45*, 7546.

(13) Later studies showed that succinic acid salts of **1** could be formed via crystallization with a continuum of stoichiometries ranging from 0.5:1 (SA:1) to 1.4:1. A detailed analytical study of the various salts was conducted and reported. See: Clawson, J. S.; Vogt, F. G.; Brum, J.; Sisko, J.; Patience, D. B.; Dai, W.; Sharpe, S.; Jones, A. D.; Pham, T. N.; Johnson, M. N.; Copley, R. C. P. *Cryst. Growth Des.* **2008**, *8*, 4120. Details of our efforts to controllably manufacture salts with various stoichiometries will be discussed in future communications.

Experimental Section

(1*R*,2*R*,4*S*,6*R*,7*R*,9*R*)-4-Ethenyl-2,4,7,14-tetramethyl-9-(methyloxy)-3-oxotricyclo[5.4.3.01,8]tetradec-6-yl Hydroxyacetate (3). Compound **2** (40 kg, 1 equiv) was dissolved in methanol (221.6 kg, 7 vol) and trimethyl orthoformate (50.4 kg, 1.3 vol) at 20 °C. Concentrated sulphuric acid (18.4 kg, 0.25 vol) was added over 15 min at <30 °C. The mixture was heated to 35 °C and stirred for 7 h. Triethylamine (29.0 kg, 1 vol) was added, and the mixture was heated to 55 °C. Water (175.2 L, 4.4 vol) and methyl isobutyl ketone (3.2 kg, 0.1 vol) were added while maintaining the temperature at 50−60 °C. The solution was cooled to 45 °C, and seed crystals (0.4 kg) were added. The solution was cooled to 40 °C and held there for 1.5 h before cooling to 30 °C over 1.5 h and holding for an additional 2.5 h. The solution was further cooled to 15 °C and held for 12 h then cooled to 0 °C for 1 h. The product was isolated by centrifuge, washed twice with water (120 L, 3 vol each), and dried under vacuum at 25 °C for 15 h to give 31.3 kg (75% yield) of compound **3** as a white powder.

^{1}H NMR δ (ppm) ($CDCl_3$, 700 MHz): 6.65 (1H, dd, J = 17.5 Hz, 10.5 Hz), 5.89 (1H, d, J = 10.5 Hz), 5.32 (1H, d, J = 10.5 Hz), 5.04 (1H, d, J = 17.5 Hz), 4.11 (2H, dd, J = 27.3 Hz, 17.5 Hz), 3.47 (1H, m), 3.23 (3H, s), 2.92 (1H, q, J = 6.3 Hz), 2.50 (1H, m), 2.01 (2H, m), 1.73 (1H, d, J = 11.2 Hz), 1.58 (2H, m), 1.46 (1H, m), 1.32 (1H, m), 1.25 (1H, m), 1.24 (3H, s), 1.20 (3H, s), 1.16 (1H, m), 1.09 (1H, m), 1.01 (3H, d, J = 6.41 Hz), 0.80 (3H, d, J = 7.0 Hz). ^{13}C NMR δ (ppm) ($CDCl_3$, 176 MHz): 215.5, 172.9, 140.5, 118.8, 83.4, 73.9, 64.5, 61.7, 57.2, 54.3, 47.9, 45.5, 45.3, 44.7, 43.6, 40.7, 31.0, 29.8, 29.0, 25.9, 20.6, 16.8 16.1.

(1*R*,2*R*,4*S*,6*R*,7*R*,9*R*)-4-Ethenyl-2,4,7,14-tetramethyl-9-(methyloxy)-3-oxotricyclo[5.4.3.0^{1,8}]tetradec-6-yl Carbamate (9). Methanol (43.6 kg) and **3** (21.8 kg, 1.0 equiv) were warmed to 40−45 °C until dissolution is observed. A solution of KOH (6.3 kg, 2.0 equiv) in water (10.9 L) was added to the methanol mixture, and the contents were heated to 60−63 °C for 2 h. The mixture was cooled to 40 °C, and heptane (89.4 kg) and water (65.4 L) were added. The mixture was stirred at 40−50 °C for 15 min, and the aqueous layer was removed. The heptane layer was washed with water (50 L) at 40 − 45 °C. Heptane was removed by vacuum distillation to a final volume of ∼40 L. *tert*-Butyl methyl ether (113 kg) was added, and the resulting solution was cooled to ∼5 °C. Chlorosulfonyl isocyanate (10.2 kg, 1.3 equiv) was added over 20 min at ∼15 °C. After 75 min, an additional portion of chlorosulfonyl isocyanate (1.6 kg, 0.2 equiv) was added to drive the reaction to completion. After stirring for an additional 30 min, water (54.5 L) was added slowly, at <30 °C. Triethylamine (5.7 kg, 2 equiv) was added at <35 °C during the addition, warmed to 45 °C, and stirred for 1 h and then at 20 °C for 12 h. The reaction was warmed to 35 °C, and the aqueous layer was removed. The organic layer was washed with water (43.6 L), and the organic layer was removed. The solution was concentrated under vacuum to a final volume of ∼44 L, and

an additional portion of heptane (29.8 kg) was added. The solution was again concentrated to ~44 L and heated to 60−65 °C, and heptane (29.8 kg) and toluene (9.4 kg) were added. The contents were stirred for 30 min at 60−65 °C and then cooled over 2 h to 0−5 °C. The reactor contents were held at 0−5 °C for 1 h, and the solids were isolated by centrifuge. The vessel and cake were rinsed with heptane (44.9 kg). The solids were dried under vacuum at ~30 °C for 12 h to yield 17.9 kg (85% yield) of compound **9** as a white solid.

^{1}H NMR δ (ppm) (DMSO-d_6, 400 MHz): 6.72 (1H, dd, J = 17.5, 10.6 Hz), 6.47 (2H, br), 5.50 (1H, d, J = 10.0 Hz), 5.24 (1H, d, J = 10.6 Hz), 4.93 (1H, d, J = 17.5 Hz), 3.36 (1H, m), 3.12 (3H, s), 2.86 (1H, q, J = 6.4 Hz), 2.31 (1H, dd, J = 15.3, 10.0 Hz), 2.04 (1H, m), 1.93 (1H, m), 1.82 (1H, m), 1.64 (1H, d, J = 11.5 Hz), 1.53 (1H, d, J = 15.5 Hz), 1.40 (2H, m), 1.24 (1H, m), 1.15 (3H, s), 1.12 (1H, m), 1.10 (3H, s), 1.07 (1H, m), 0.90 (3H, d, J = 6.4 Hz), 0.81 (3H, d, J = 7.0 Hz). ^{13}C NMR δ (ppm) (DMSO-d_6, 100 MHz): 214.5, 156.0, 140.9, 117.6, 82.4, 69.8, 63.2, 56.3, 53.3, 47.0, 44.8, 44.2, 42.8, 39.6, 30.1, 28.9, 28.3, 25.4, 20.3, 16.2, 15.4.

***trans*-4-({[(1,1-Dimethylethyl)oxy]carbonyl}amino)cyclohexyl (1*R*,2*R*,4*S*,6*R*,7*R*,9*R*)-4-Ethenyl-2,4,7,14-tetramethyl-9-(methyloxy)-3-oxotricyclo[5.4.3.0^{1,8}]tetradec-6-yl Imidodicarbonate (7).** *N*-Methylpyrrolidinone (82.4 kg), **9** (40.0 kg, 1.0 equiv) and **10** (40.0 kg, 1.2 equiv) were slurried together for 30 min and then cooled to 5 °C. A solution of sodium *tert*-pentoxide (29.2 kg, 2.5 equiv) in NMP (123.6 kg) was added to the slurry containing **9** and **10** over 30 min. The reactor containing the pentoxide base was rinsed with NMP (41.2 kg), and the rinse was added to the reactor vessel. After 30 min, a solution of citric acid (0.76 kg) and water (7.2 L) was added to the reaction, and the resulting mixture was warmed to ~25 °C and stirred for 15 min until dissolution was observed. The mixture was added over 20 min to a second vessel containing a solution of citric acid (69.4 kg) and water (650 L). The resulting slurry was filtered via centrifuge in six separate portions and washed with water (at least 133 L per portion), and the product (compound **7**, 258.5 kg 'wet') was stored and used without further drying in the next step. Yield was assumed to be 100% for the purposes of calculating charges in stage 4.

^{1}H NMR δ (ppm) ($CDCl_3$, 400 MHz): δ 6.70 (1H, dd, J = 16.0, 8.0 Hz), 5.74 (1H, d, J = 8.0 Hz), 5.28 (1H, d, J = 12.0 Hz), 4.99 (1H, d, J = 16.0 Hz), 4.70 (1H, m), 4.45 (1H, d, J = 6.6 Hz), 3.45 (2H, m), 3.23 (3H, s), 2.88 (1H, m), 2.48 (1H, m), 2.21 (1H, m), 2.03 (6H, m), 1.70 (3H, m), 1.57 (6H, m), 1.46 (9H, s), 1.25 (3H, s), 1.20 (3H, s), 1.17 (1H, m), 1.01 (3H, d, J = 4.0 Hz), 0.87 (3H, d, J = 4.0 Hz). ^{13}C NMR δ (ppm) ($CDCl_3$, 100 MHz): 215.1, 155.2, 150.2, 150.1, 140.2, 118.4, 83.0, 79.3, 74.4, 74.0, 64.0, 56.7, 53.7, 48.4, 47.5, 45.2, 44.8, 44.0, 43.2, 40.2, 30.6, 29.9, 29.4, 28.5, 28.3, 25.6, 20.3, 17.6, 16.5, 15.7.

***trans*-4-Aminocyclohexyl (1*S*,2*R*,3*S*,4*S*,6*R*,7*R*,8*R*)-4-Ethenyl-3-hydroxy-2,4,7,14-tetramethyl-9-oxotricyclo[5.4.3.0^{1,8}]-tetradec-6-yl Imidodicarbonate Bis-(2-propanol) Solvate (11).** A reactor was charged with toluene (262 L, 4 vol, based on wt/wt assay of compound **7** (256 kg crude, 65.5 kg at 100%, 1 equiv)). The mixture was heated to 60−65 °C and held for 30−40 min. Stirring was stopped to allow phase separation, and the bottom aqueous portion was discarded. To the top organic layer was added water (196.8 L), and the mixture was stirred at 70−75 °C for 20−30 min. Stirring was stopped to allow phase separation, and the bottom aqueous portion was discarded. The contents in the reactor were cooled to 10−15 °C, and conc HCl (116.1 kg) was added over 30−40 min at <30 °C. Once the HCl addition was complete, the reaction temperature was raised to 20−25 °C, and the reaction was stirred 2 h. The agitation was stopped, and the lower aqueous layer containing the product was separated. To the top organic portion was added conc HCl (19.7 kg, 0.27 vol), and the mixture was stirred for ~10 min and settled. The bottom, aqueous layer was combined with the original aqueous acid layer, and the organic layer was discarded. The combined aqueous solutions were added over 1.5 h into a second vessel containing a mixture of ammonium hydroxide (30% aqueous, 137.8 kg), water (65.5 L), 2-PrOH (65.5 L), and ethyl acetate (295.9 kg) that has been cooled to ~15 °C. The temperature in the vessel was maintained at <30 °C during the addition, and the final pH was >9 after complete addition. After stirring the mixture at 20−25 °C for 0.5 h, the bottom aqueous layer was separated and discarded. To the organic layer was added water (196.8 L), and the mixture was stirred at 20−25 °C for 0.5 h. The aqueous layer was discarded, and the organic portion was concentrated to a final volume of ~200 L. 2-PrOH (257.8 kg) was added, and the mixture was concentrated under vacuum to a final volume of ~330 L. The mixture was cooled to 0−5 °C over 2 h and held at this temperature for 1 h. The mixture was filtered via centrifuge and the wet cake rinsed with cold 2-PrOH (103 kg). The solid product was dried under vacuum (~60 °C) to a final LOD of <20% to give 55.1 kg (83% yield) of product **11**.

^{1}H NMR δ (ppm) (DMSO-d_6, 400 MHz): 6.22 (1H, dd, J = 17.7, 11.5 Hz), 5.46 (1H, d, J = 8.1 Hz), 5.10 (1H, dd, J = 17.5 Hz, 1.7 Hz), 5.05 (1H, dd, J = 11.0 Hz, 1.7 Hz), 4.48 (1H, m), 4.26 (6H, br), 3.77 (2H, m), 3.42 (1H, d, J = 5.5 Hz), 2.57 (1H, m), 2.35 (1H, m), 2.18 (1H, m), 2.08 (3H, m), 1.88 (2H, m), 1.76 (2H, m), 1.64 (2H, m), 1.46 (2H, m), 1.37 (3H, s), 1.28 (6H, m), 1.13 (2H, m), 1.06 (3H, s), 1.03 (12H, d, J = 6.1 Hz), 0.81 (3H, d, J = 6.8 Hz), 0.63 (3H, d, J = 6.6 Hz). ^{13}C NMR δ (ppm) (DMSO-d_6, 100 MHz): 217.1, 150.8, 150.5, 140.9, 115.2, 73.4, 72.7, 69.9, 62.0, 57.4, 49.0, 45.0, 44.0, 43.8, 41.6, 36.3, 34.0, 33.2, 30.1, 29.8, 28.2, 26.6, 25.5, 24.5, 16.1, 14.7, 11.5.

***trans*-4-Aminocyclohexyl (1*S*,2*R*,3*S*,4*S*,6*R*,7*R*,8*R*)-4-Ethenyl-3-hydroxy-2,4,7,14-tetramethyl-9-oxotricyclo[5.4.3.0^{1,8}]-tetradec-6-yl Imidodicarbonate Succinic Acid Salt (1A).** A reactor was charged with **11** (2.2 kg of the bis-(2-propanol) solvate, 1.8 kg of **1** based on wt/wt assay), 2-PrOH (4.4 L), and water (1.1 L). Succinic acid (658 g, 1.6 equiv) was charged, and the contents of the reactor were stirred

and heated to 70−75 °C until a clear solution was obtained. The solution was filtered through a 1 μm in-line filter into a crystallization reactor. The original reactor was rinsed with 2-PrOH (5.5 L) that was then sent through the filter and into the crystallization reactor. The contents of the crystallization reactor were heated to 70−75 °C to ensure complete dissolution and then cooled to ∼65 °C over 15 min and seeded with 18 g (1.0 wt %) of compound **1A** seeds that were suspended in 2-PrOH (64 mL). The slurry was held at ∼65 °C for 30−60 min and then cooled to 20 °C over 1 h. Additional 2-PrOH (11.0 L) was then added to the slurry over 30 min, and the mixture was cooled to 0−5 °C over 1 h. The product was isolated by filtration, rinsed with 2-PrOH (7.0 L), and dried under vacuum at 40−60 °C for ∼24 h. The product weighed 2.03 kg (92% yield).

^{1}H NMR δ (ppm) (DMSO-d_6, 700 MHz): 9.20 (5H, b), 6.20 (1H, dd, J = 17.7, 11.2 Hz), 5.45 (1H, d, J = 8.3 Hz), 5.09 (1H, dd, J = 17.5, 1.8 Hz), 5.04 (1H, dd, J = 11.2, 1.8 Hz), 4.48 (1H, m), 3.41 (1H, d, J = 5.8 Hz), 2.98 (1H, m), 2.36 (1H, s), 2.24 (4H, s), 2.17 (1H, m), 2.07 (3H, m), 1.95 (4H, m), 1.65 (1H, m), 1.61 (1H, m), 1.48 (1H, m), 1.38 (1H, m), 1.36 (5H, s), 1.24 (5H, m), 1.05 (3H, s), 1.00 (1H, m), 0.80 (3H, d, J = 7.0 Hz), 0.61 (3H, d, J = 7.0 Hz). ^{13}C NMR δ (ppm) (DMSO-d_6, 176 MHz): 217.1, 175.5, 150.7, 150.5, 140.9, 115.2, 72.7, 72.3, 70.0, 57.3, 47.9, 44.9, 43.9, 43.8, 41.6, 36.3, 34.0, 32.2, 30.1, 28.8, 28.3, 28.2, 26.6, 24.5, 16.1, 14.7, 11.5.

Acknowledgment

We thank Thomas Wrzosek and James Ward for their assistance in analyzing and interpreting the results of the DoE studies.

Supporting Information Available

Copies of the NMR spectra of all intermediates and final product as well as the raw data for the DoE study. This material is available free of charge via the Internet at http://pubs.acs.org.

Received for review April 23, 2009.

OP900104G